Available online at www.sciencedirect.com

ScienceDirect

Karbala International Journal of Modern Science 2 (2016) 69–77

http://www.journals.elsevier.com/karbala-international-journal-of-modern-science/

# Spectral investigations to the effect of bulk and nano ZnO on peanut plant leaves

S. Suresh [a,b,*], S. Karthikeyan [a,c], K. Jayamoorthy [d]

[a] *Research and Development Center, Bharathiar University, Coimbatore 641046, Tamilnadu, India*

[b] *Department of Physics, St.Joseph's College of Engineering, Chennai 600119, Tamilnadu, India*

[c] *Department of Physics, Dr. Ambedkar Government Arts College, Chennai 600039, Tamilnadu, India*

[d] *Department of Chemistry, St.Joseph's College of Engineering, Chennai 600119, Tamilnadu, India*

Received 22 December 2015; revised 21 January 2016; accepted 22 January 2016

Available online 6 April 2016

**Abstract**

The potential variation in peanut plant leaves were examined by the application of bulk and nano ZnO through presowing method. ZnO nanoparticles synthesized by chemical route and were characterized using x-ray diffraction, atomic force, scanning electron and transmission electron microscopy. ZnO nanoparticles and bulk counterpart are applied to the peanuts by presowing method in two concentrations of 500 ppm and 4000 ppm. Fourier transform infrared spectra exhibit variation in most prominent peaks ~2923, ~1636, ~1033 $cm^{-1}$ due to ZnO stress in both nano and bulk form, which was supported from the calculated mean ratio of the peak intensities for various frequency region and total band area calculation for various band region. The infrared spectra were further processed by de-convolution and curve fitting analysis to examine the variation in secondary structure protein of leaf samples stressed with ZnO bulk and nanoparticles. Multivariate analyses shows the successive factors account for decreasing amounts of residual variance using two factors for the wave numbers 1633, 1648, 1656, 1666, 1673 and 1684 $cm^{-1}$ assigned to protein secondary structure of leaf samples.



*Keywords:* Peanut plant; Zinc oxide solutions; FT-IR; Pre-sowing method

## 1. Introduction

Micronutrients like zinc, iron, magnesium, manganese, etc. was used in agriculture at low concentration for potential growth of plants. Even though micronutrients required for plant growth, become toxic when the concentration exceeds the permissible level. Lead, mercury and cadmium are some of the non-essential elements which are highly toxic even at lower concentration [1,2]. Zinc is an essential element for normal plant growth and it is widely used for many applications [3–10]. Zinc deficiency is most common in many plants like corn, sorghum, cotton, etc. The first obvious symptom of zinc deficiency is interveinal chlorosis of the upper (youngest) leaves. Afterwards, shoot growth slows down; giving the affected plant parts a rosette-like appearance. Higher uptakes of other nutrients are also known to increase the demand of Zn

* Corresponding author. Research and Development Center, Bharathiar University, Coimbatore 641046, Tamilnadu, India. Tel.: +91 9884633846.

*E-mail addresses:* profsuresh1@gmail.com (S. Suresh), physicskarthik@gmail.com (S. Karthikeyan).

Peer review under responsibility of University of Kerbala.

http://dx.doi.org/10.1016/j.kijoms.2016.01.005

[11]. The toxic effects of metal oxide also plays important role in plant growth. Nanoparticles can serve as "magic bullets", containing herbicides, nano-pesticide fertilizers or genes, which target specific cellular organelles in plant to release their content. Several works focused to stimulate the seed germination using nanoparticles and its use as a source of micronutrients. Presoaking was commonly used to reduce the time between seed sowing and seedling emergence and to synchronize emergence. Presoaking seeds have important role in increasing the yield of different crops in relation to enhance 37, 40, 70, 22, 31, 56, 50 and 20.6% in wheat, barley, upland rice, maize, sorghum, pearl millet, and chick pea respectively [12,13]. In this work the effect on biochemical constituents and metal concentration in peanut plant leaves (collected after 30 days of sowing) due to presoaking peanut seeds in zinc oxide bulk and nanoparticle suspension for 10 hours was studied.

## 2. Experimental

### 2.1. Synthesis of ZnO nanoparticles

The zinc oxide nanoparticle was synthesized using chemical precipitation method. Zinc nitrate is used as the precursor material and is taken as solution in a beaker. The zinc nitrate solution is stirred well using a magnetic stirrer and ammonium hydroxide solution is added in drops to get zinc hydroxide precipitate. The solution was continuously stirred to avoid agglomeration of precipitated particles. The precipitate is then washed several times with distilled water and ethanol further annealed at 400 °C for 4 h to remove water content and form zinc oxide (ZnO) nanoparticles. The annealed sample analyzed for phase confirmation and particle size using XRD, SEM, AFM and HR-TEM techniques [14].

### 2.2. Seed preparation and presoaking

The peanut seeds obtained from Regional agricultural research institute, Virudhachalam. The seeds were sterilized in a 5% sodium hypochloride solution for 5–10 min, and then rinsed thoroughly several times with deionized water. The seeds were treated with two different concentration of bulk and nano zinc oxide suspension (500 & 4000 ppm) for a time period of 10 h. Later the seeds sowed in separate pots for each concentration of both nano and bulk zinc oxide. A total of three replicates were chosen for each physiological measurement (at an average of three plants per replica) where the results were presented as mean ± standard deviation (SD) [15].

### 2.3. FT-IR spectral analysis

The leaf samples were sectioned from the plant collected after 30 days of sowing. All the leaf samples were oven dried at 100 °C for 48 h to remove moisture and ground to fine powder. The infrared spectra of leaves were recorded using KBr pellet technique in BRUKER IFS 66V model FT-IR spectrometer in the region 4000–400 $cm^{-1}$. Each sample was scanned under the same conditions with three different pellets. These replicates were averaged and then used. The spectra were analyzed using Origin 8.0 software (OriginLab Corporation, Massachusett, USA). For discussion the samples was named $L^1$, $L^2$, $L^3$ and $L^4$ where, $L^1$ – Leaf samples of plant seeds soaked in 500 ppm zinc oxide bulk suspension collected after 30 days of sowing, $L^2$ – Leaf samples of plant seeds soaked in 4000 ppm zinc oxide bulk suspension collected after 30 days of sowing, $L^3$ – Leaf samples of plant seeds soaked in 500 ppm zinc oxide nano suspension collected after 30 days of sowing, $L^4$ – Leaf samples of plant seeds soaked in 4000 ppm zinc oxide nano suspension collected after 30 days of sowing.

### 2.4. Statistical analysis

All statistical analysis was performed using SPSS 16.0 software. Pearson's correlation matrix was calculated for secondary structure protein of leaf samples. Principle component analysis was carried out to find the factors which influence the variation in protein content among the leaf samples treated with bulk and nano zinc oxide in comparison with control sample. Graphical work was carried out using Originsoftware 8.0.

## 3. Results and discussion

### 3.1. XRD, SEM, AFM and TEM analyses of zinc oxide nanoparticles

Fig. 1 visualizes the XRD pattern of zinc oxide. The formation of zinc oxide phase in 400 °C annealed sample was confirmed by an X-ray diffractometer. The average grain sizes were determined from the XRD patterns using the Debye-scherrer formula. The average particle size of the zinc oxide nanoparticle was found to be 23.90 nm. The peaks were matched using JCPDS software and it was well matched with the zinc

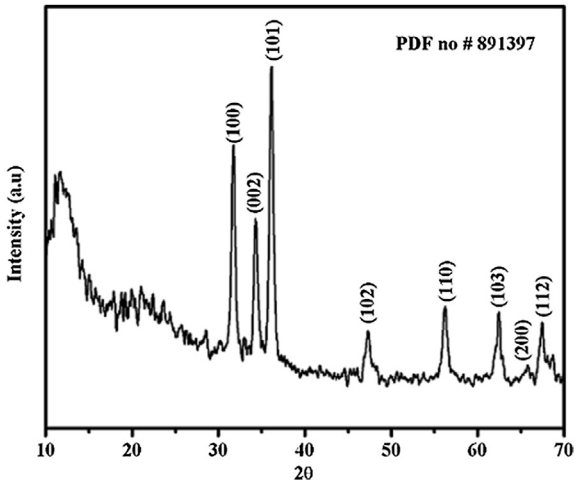


Fig. 1. XRD pattern of zinc oxide nanoparticles.

oxide (ZnO) of file no "Pdf # 891397". The SEM image confirms the uniformity of phase formation and the particle size of the zinc oxide nanoparticle. Fig. 2 visualize the SEM images of zinc oxide.

The 2D and 3D atomic force microscopy image of zinc oxide nanoparticle confirms the particle size exist in nano range. The average particle size of the zinc oxide calculated from XRD results nearly match with AFM results as shown in the Fig. 3. Fig. 4 shows the TEM image and selected area electron diffraction (SAED) pattern of zinc oxide nanoparticle. The image clearly shows the particle sizes are in nanometer and the SAED pattern explains the polycrystalline nature of zinc oxide nanoparticle.

### 3.2. FT-IR spectral studies of leaf samples

The tentative frequency assignment of averaged spectra for the peanut leaf samples collected after 30 days of sowing was tabulated in Table 1 and spectra shown in Fig. 5. The strong characteristic band at ~3415 $cm^{-1}$ to ~3422 $cm^{-1}$ in control, $L^1$, $L^2$, $L^3$ and $L^4$ leaf samples was assigned to the O–H Stretching/ N–H stretching of amide A. The characteristic band at ~2955 $cm^{-1}$ due to $CH_3$ – asymmetric stretching does not varies in all the leaf samples whereas $CH_2$ asymmetric stretching band at ~2921 $cm^{-1}$ shows decreased intensities in $L^2$, $L^3$ and $L^4$ samples but $L^1$ sample has no variation compared to control leaf sample. The $CH_2$ symmetric stretching of lipid, protein band at ~2851 $cm^{-1}$ show decreased intensities in $L^3$ & $L^4$ but found increased in $L^1$, also no significant change observed in $L^2$ leaf sample. The weak band at ~1736 $cm^{-1}$ assigned to carbonyl C=O stretch: lipids, chlorophyll, were found with elevated intensities in $L^1$, $L^3$ & $L^4$ leaf samples. The stretching vibration of free keto group at ~1725 $cm^{-1}$ show elevated intensity in $L^1$, $L^3$ & $L^4$ leaf samples also there exist an 8 $cm^{-1}$ shift in band observed in all samples except $L^4$ sample where the shift was 3 $cm^{-1}$. The amide I protein is present in all the samples which was observed from the very strong band at ~1630–1636 $cm^{-1}$. The band at ~1547 $cm^{-1}$ gives the presence of amide II in all leaf samples and an increased intensity was found all leaf samples suggesting the increase in protein content of leaf sample. The bands at ~1426, ~1383 and ~1255 $cm^{-1}$ in control leaf sample is assigned to C–N stretching/in-plane OH bending, $CH_3$ symmetric bending; protein and C–O stretching (ethers)/C–N stretching (amines) respectively. In these spectral regions an elevated intensities observed in $L^1$ and $L^4$ leaf samples alone which indicates the increase in amide III protein with respect to control leaf sample. The variation in intensities of bands from ~1156 to 1033 $cm^{-1}$ indicates the variation in carbohydrates and all other nucleic acids in all leaf samples compared to control leaf sample. The intensity of band at ~1156 $cm^{-1}$ corresponds to CH deformation, C–O, C–C stretching

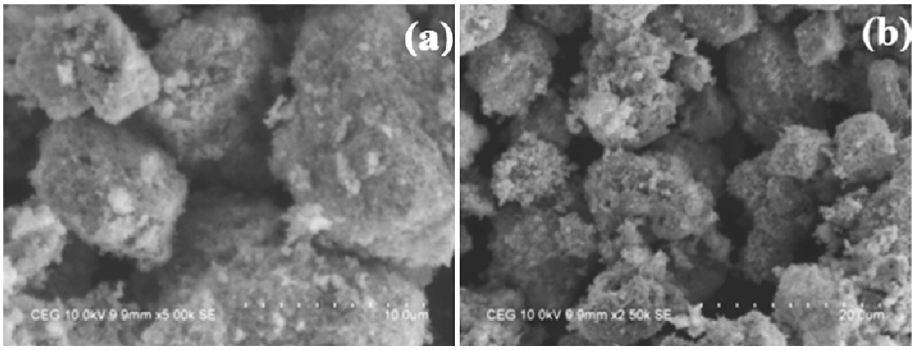


Fig. 2. SEM images of zinc oxide nanoparticles a) 10 μm image b) 20 μm image.

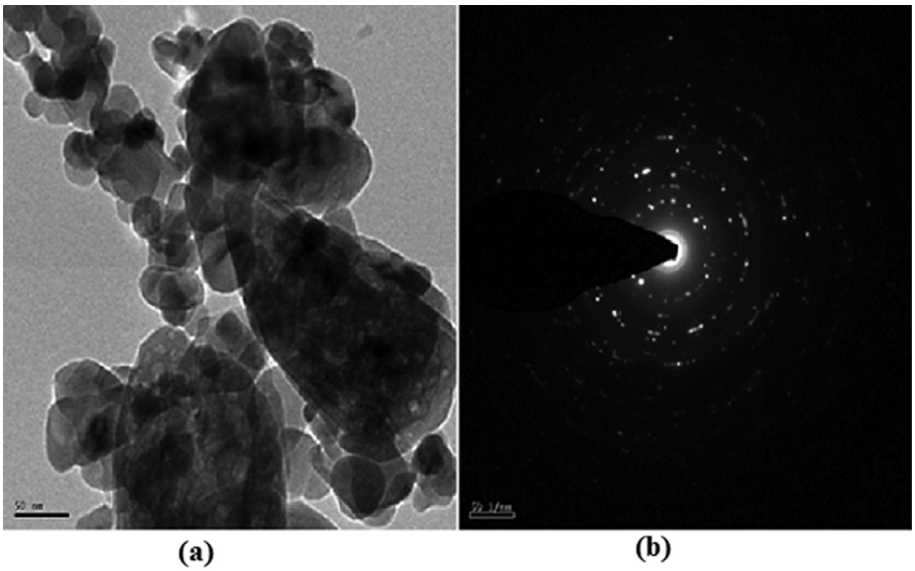


Fig. 3. TEM images of zinc oxide nanoparticles a) 100 nm image b) SAED pattern.

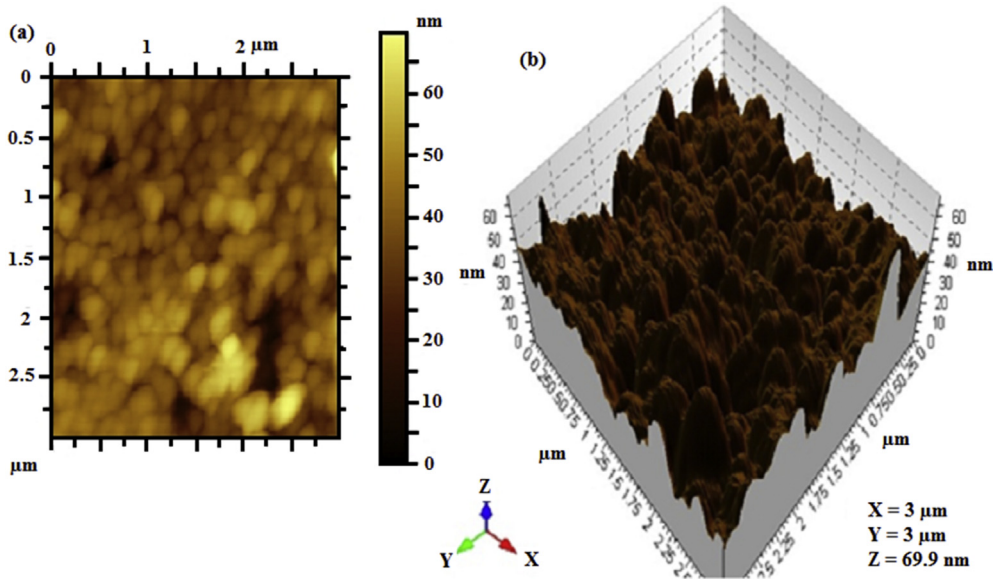


Fig. 4. The atomic force microscopy images of zinc oxide nanoparticles a) 2D image b) 3D image.

(carbohydrates) was decreased in $L^3$ leaf sample but remains same in other leaf samples compared to control leaf sample. The intensities of characteristic band at ~1105 and ~1070 $cm^{-1}$ were found with elevated intensities in $L^1$ and $L^4$ leaf samples alone. The characteristic band at ~1061 and ~1070 $cm^{-1}$ assigned to $PO_2^-$ symmetric stretch: mainly nucleic acids were absent in $L^1$ and $L^3$ leaf sample respectively. Also the intensity of band at ~1061 $cm^{-1}$ was found increased in $L^2$ and $L^4$ leaf samples. The characteristic band at ~1033 $cm^{-1}$ assigned to C–O stretching/C–O bending of the C–O–H carbohydrate, the intensities of which found increased in $L^2$ and $L^4$ leaf samples but decreased in $L^2$ leaf sample. The characteristic band at ~1033 $cm^{-1}$ exhibit a 11 $cm^{-1}$ shift in $L^1$ leaf sample compared to control sample. A very weak band at 962 $cm^{-1}$ of $C-N^+-C$ symmetric stretch of nuclei acids present in control and $L^2$ leaf

Table 1
Frequency assignment of FT-IR spectra for the peanut leaf samples collected after 60 days.

| Control | Zinc oxide bulk | | Zinc oxide nano | | Tentative frequency assignment |
|---|---|---|---|---|---|
| | $L^1$ | $L^2$ | $L^3$ | $L^4$ | |
| 3415(vs) | 3419(vs) | 3419(vs) | 3420(vs) | 3422(vs) | Bonded O–H Stretching/N–H stretching |
| 2955(m) | 2954(m) | 2955(m) | 2956(m) | 2955(m) | $CH_3$ symmetric stretching; lipid, protein |
| 2921(vs) | 2921(vs) | 2919(s) | 2919(m) | 2919(m) | $CH_2$ asymmetric stretching; mainly lipid, protein |
| 2851(m) | 2850(s) | 2850(m) | 2850(w) | 2850(w) | $CH_2$ symmetric stretching; lipid, protein |
| 1736(w) | 1734(m) | 1734(w) | 1734(m) | 1737(m) | Carbonyl C=O stretch: lipids |
| 1725(w) | 1717(m) | 1717(w) | 1717(m) | 1722(m) | Stretching vibration of free keto group |
| 1630(vs) | 1635(vs) | 1635(vs) | 1635(vs) | 1631(vs) | Amide I: C=O stretching of proteins |
| 1547(m) | 1540(vs) | 1540(s) | 1540(s) | 1551(s) | Amide II: N–H Bending/C–N stretching of proteins |
| 1426(m) | 1418(s) | 1419(m) | 1419(m) | 1426(s) | C–N stretching/in-plane OH bending |
| 1383(m) | 1384(s) | 1384(m) | 1387(m) | 1384(s) | $CH_3$ symmetric bending; protein |
| 1255(w) | 1259(m) | 1262(vw) | 1261(w) | 1257(m) | C–O stretching (ethers)/C–N stretching (amines) |
| 1156(m) | 1151(m) | 1153(m) | 1154(w) | 1153(m) | CH deformation, C–O, C–C stretching (carbohydrates) |
| 1105(m) | 1101(s) | 1098(m) | 1103(m) | 1104(s) | |
| 1070(m) | 1071(s) | 1070(m) | – | 1072(s) | PO2 – symmetric stretch: mainly nucleic acids |
| 1061(m) | – | 1060(s) | 1061(m) | 1057(s) | |
| 1033(m) | 1022(s) | 1034(s) | 1033(m) | 1032(vs) | C–O stretching/C–O bending of the C–O–H carbohydrates |
| 962(vw) | – | 962(vw) | – | – | $C–N^+$-C symmetric stretch: nuclei acids |
| – | – | – | – | 668(s) | $CH_2$ bending, carbohydrates, proteins and lipids (sterols of fatty acids) |

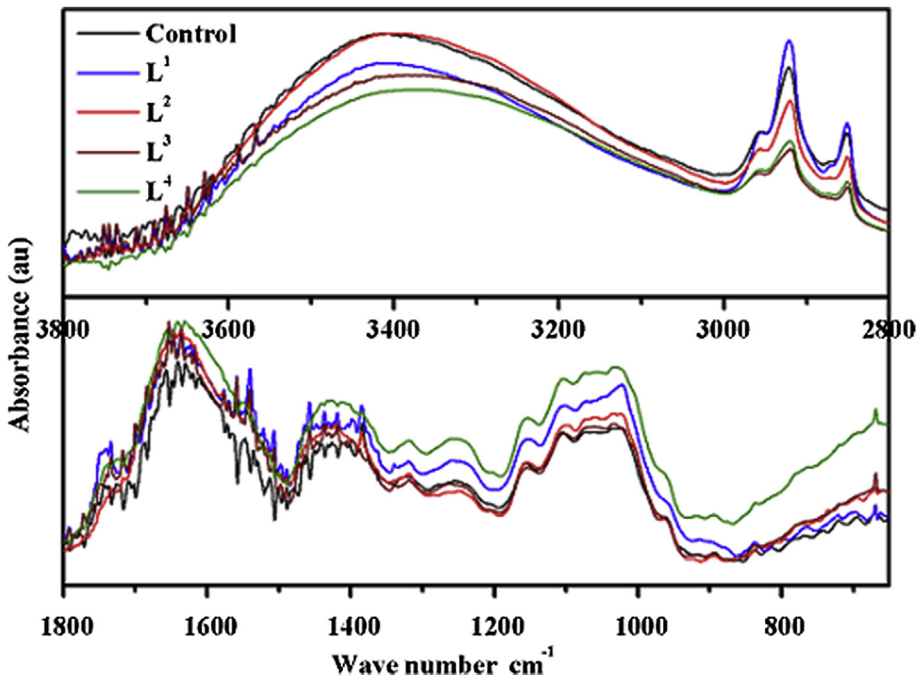


Fig. 5. FT-IR spectra of control, $L^1$, $L^2$, $L^3$ & $L^4$ leaf samples.

sample alone and were absent in all other leaf samples. The FTIR results shows that the presoaking of peanut seeds with ZnO bulk and nanoparticle suspensions of concentration 500 and 4000 ppm might have considerable influence on the protein, chlorophyll, carbohydrate and other biochemical constituents of leaf samples collected after 30 days of sowing.

The total band area calculation for various spectral regions gives the changes in biochemical constituents of leaf samples directly from raw spectra. The spectral

Table 2
The total band area calculated for all the iron oxide soaked samples and compared with the control leaf sample.

| Spectral Region ($cm^{-1}$) | Control | $L^1$ | $L^2$ | $L^3$ | $L^4$ |
|---|---|---|---|---|---|
| 3200–3450 | 409.92 ± 3.126 | 321.48 ± 2.944–21.58 | 426.20 ± 3.562 +3.97 | 327.72 ± 2.823–20.04 | 337.98 ± 3.210–17.55 |
| 2800–3000 | 145.64 ± 1.257 | 134.04 ± 1.087–7.96 | 131.41 ± 0.945–9.77 | 96.01 ± 0.651–34.07 | 59.80 ± 0.664–58.94 |
| 1800–1500 | 135.35 ± 0.541 | 167.93 ± 0.723 +24.06 | 159.91 ± 0.771 +18.17 | 163.20 ± 0.455 +20.58 | 176.33 ± 0.365 +30.28 |
| 1300–1450 | 66.63 ± 1.203 | 75.14 ± 0.884 +12.85 | 69.02 ± 0.956 +3.65 | 65.46 ± 1.086 −1.75 | 91.61 ± 1.412 +37.56 |
| 1000–1200 | 96.02 ± 4.122 | 130.11 ± 6.445 +35.58 | 102.61 ± 4.862 +6.89 | 99.94 ± 4.354 +4.11 | 150.32 ± 5.009 +56.60 |

The values are the mean ± S.E for each group (n = 9). Comparisons were done by Students t-test. The degree of significance was $p < 0.05$.

region between 3450 and 3200 $cm^{-1}$, 3000 and 2800 $cm^{-1}$, 1800 and 1500 $cm^{-1}$, 1450 and 1300 $cm^{-1}$, 1200 and 1000 $cm^{-1}$ were selected to analyze amide A and B protein, lipids, proteins, cellulose and lignin, carbohydrates respectively [16]. The Table 2 shows the total band area calculated for control, $L^1$, $L^2$, $L^3$ and $L^4$ leaf samples. The total band area of the spectral region 3450–3200 $cm^{-1}$ region found decreased by 21.58%, 20.04%, and 17.55% in $L^1$, $L^3$ & $L^4$ leaf samples respectively but in $L^2$ sample increased slightly by 3.97% compared to the control leaf sample. This shows the variation in amide-A protein in leaf samples. The lipid content of leaf samples were analyzed by calculating the total band area in the region 3000–2800 $cm^{-1}$, the results shows decrease in band area by 7.96%, 9.77%, 34.07% and 58.94% in $L^1$, $L^2$, $L^3$ & $L^4$ leaf samples respectively compared to control leaf sample. The amide I and amide II protein content in leaf samples found increased compared to control leaf sample, which evidenced by increase in total band area calculated in the band region 1800–1500 $cm^{-1}$. The variation of cellulose and lignin were estimated by the total band area calculated in the band region 1450–1300 $cm^{-1}$ was found increased in $L^1$, $L^2$ & $L^4$ leaf samples but slightly decreases in $L^3$ by 1.75%. The carbohydrate content in all leaf samples found increased compared to control sample and the maximum variation was found in $L^4$ sample by 56.60%. Thus the total band area calculations in various band region explains the variation in proteins, lipid, carbohydrates, nuclei acids and other biochemical constituents due to the presoaking of peanut seeds with zinc oxide bulk and nano suspension.

The FT-IR spectra were recorded with care by preparing the pellet of all the samples taking same weight during pelletizing, so the relative biochemical change is assessed by calculating the mean ratio of the peak intensities corresponding to various wavenumber. The mean ratio of the peak intensities of the bands at 1540 $cm^{-1}$ and at 3347 $cm^{-1}$ ($I_{1540}/I_{3347}$) was used as an indicator of the relative concentration of the protein in the leaf samples (Table 3). The calculated ($I_{1540}/I_{3347}$) ratios of the leaf samples increased compared to control sample. The maximum variation in relative protein was found in $L^1$ leaf sample by 74.58% compared to control leaf sample. The mean ratios of the absorption intensity of the methyl band and methylene band ($I_{2954}/I_{2850}$) of samples $L^2$, $L^3$and $L^4$ are 1.066 ± 0.002, 1.161 ± 0.003, and 1.131 ± 0.004 respectively, which correspond to an increase of 5.64%, 15.01% and 12.08% respectively but the mean intensity ratio found to decrease by 7.12% in $L^1$ leaf sample. The increase in the ratios indicates the number of methyl groups in protein fibers is more compared to methylene groups in these leaf samples.

The mean ratio of the intensities of the bands at 1540 $cm^{-1}$ and 1635 $cm^{-1}$ could be attributed to change in the composition of the whole protein pattern ($I_{1540}/I_{1635}$). The calculated mean ratio of intensities of $L^1$, $L^2$ and $L^3$ leaf samples are 0.834 ± 0.009, 0.676 ± 0.007 and 0.754 ± 0.007, which attribute to

Table 3
Mean ratio of peak intensities of the bands at different wave numbers.

| Ratio of bands | Control | $L^1$ | $L^2$ | $L^3$ | $L^4$ |
|---|---|---|---|---|---|
| $I_{1540}/I_{3347}$ | 0.534 ± 0.011 | 0.933 ± 0.008 +74.58 | 0.663 ± 0.003 +24.10 | 0.869 ± 0.005 +62.62 | 0.778 ± 0.012 +45.70 |
| $I_{2954}/I_{2850}$ | 1.006 ± 0.005 | 0.937 ± 0.004–7.12 | 1.066 ± 0.002 +5.64 | 1.161 ± 0.003 +15.01 | 1.131 ± 0.004 +12.08 |
| $I_{1540}/I_{1635}$ | 0.629 ± 0.014 | 0.834 ± 0.009 +34.11 | 0.676 ± 0.007 +8.71 | 0.754 ± 0.007 +21.36 | 0.597 ± 0.015–3.97 |
| $I_{1071}/I_{1540}$ | 1.049 ± 0.012 | 0.828 ± 0.020–21.04 | 0.902 ± 0.012–13.96 | 0.785 ± 0.014–25.15 | 1.315 ± 0.010 +25.37 |
| $I_{1734}/I_{1430}$ | 0.653 ± 0.007 | 0.860 ± 0.005 +31.70 | 0.548 ± 0.008–16.09 | 0.812 ± 0.010 +24.31 | 0.609 ± 0.009–6.67 |
| $I_{1734}/I_{1540}$ | 0.617 ± 0.023 | 0.621 ± 0.018 +0.57 | 0.466 ± 0.012–24.42 | 0.609 ± 0.011–1.37 | 0.683 ± 0.009 +10.58 |

The values are the mean ± S.E for each group (n = 9). Comparisons were done by Students t-test. The degree of significance was $p < 0.05$.

the increase in whole protein of 34.11%, 8.71%, and 21.36% in these samples respectively whereas the total protein of $L^4$ leaf sample shows slight decrease of 3.97% compared to control leaf sample. From these results it was observed that the total protein of leaf samples increases when peanut seeds presoaked in 500 ppm of bulk and nano zinc oxide suspension and 4000 ppm concentration of bulk, but decreases when peanut seeds primed with 4000 ppm nano zinc oxide suspension.

The mean ratio of peak intensities of the bands ($I_{1071}/I_{1540}$) attributed to glycoprotein was found to be 0.828 ± 0.020, 0.902 ± 0.012, 0.785 ± 0.014 and 1.315 ± 0.010 for $L^1$, $L^2$, $L^3$ and $L^4$ respectively. The glycoprotein of leaf samples $L^1$, $L^2$ and $L^3$ found to decrease by 21.04%, 13.96%, and 25.15% respectively, whereas $L^4$ sample exhibit increased glycoprotein by 19.83% compared to control leaf sample. The lipid, chlorophyll variation was analyzed from the calculated mean ratio of peak intensities of the bands ($I_{1734}/I_{1430}$), which found decreased by 16.09% and 6.67% in $L^2$ and $L^4$ leaf samples respectively but an increase of 31.70% and 24.31% found in $L^1$ and $L^3$ leaf samples compared to the control sample. The increase in ratio suggested that lipids are being oxidized in $L^1$ and $L^3$ leaf samples. Since oxidation can cause an increase in carbonyls and a degradation of lipids, both of these changes could be contributed to the elevated ratio which in turn affects the chlorophyll. The mean ratio of peak intensities of bands ($I_{1734}/I_{1540}$) shows the variation of chlorophyll with that of amide II protein. The mean ratio of peak intensities of leaf samples $L^1$, $L^2$, $L^3$ and $L^4$ are 0.621 ± 0.018, 0.466 ± 0.012, 0.609 ± 0.011 and 0.683 ± 0.009 respectively whereas the mean ratio intensity of control peak sample is 0.617 ± 0.023, which reflects that $L^1$ and $L^4$ leaf samples found increased by 0.57% and 10.58% respectively but it decreased in $L^2$ and $L^3$ leaf samples by 24.42% and 1.37% respectively.

To study the secondary structure of proteins in the leaf samples, further analysis was carried out by resolving the amide I band using the curve fitting method. To find out the number of peaks in the amide I region for curve-fitting process, the second derivative spectra were calculated using Origin 8.0 software (Savitsky–Golay as a derivative operation) in the amide I region (1600–1700 $cm^{-1}$). The underlying bands of amide I band as deduced by curve fitting analysis for the control and leaf samples grown by presoaking peanut seeds with two concentrations of bulk and nano zinc oxide suspensions were tabulated in Table 4. The band around 1633 $cm^{-1}$ is assigned for β − sheet of secondary structure of protein and its integrated band area is found to increase in all the leaf samples by 40.77%, 18.26%, 152.23% and 126.17% respectively when compared with control leaf sample. This indicates the peanut seeds soaked in zinc oxide nanoparticle suspension show a steep increase in β − sheet of secondary structure of protein whereas it increased slightly in zinc oxide bulk suspension. Also the increase in β − sheet is more in 500 ppm suspension of both bulk and nano zinc oxide compared to 4000 ppm concentration. The random coil of the secondary structure of protein was observed from the peak centered at 1648 $cm^{-1}$ shows increase in band area of all the samples considerably expect $L^2$ sample where it found decreased slightly by 0.82%. The band at 1656 $cm^{-1}$ is due to α − helix of protein secondary structure which shows a steep increase in band area of $L^1$, $L^2$, $L^3$ and $L^4$ leaf samples by 222.12%, 135.80, 88.41% and 234.72% respectively. The bands centered around 1666, 1673 and 1684 $cm^{-1}$ were assigned for the β − turn of the secondary protein structure (Table 4). The integrated band area of 1666 and 1673 $cm^{-1}$ found to increase in all leaf samples. The integrated band area of 1684 $cm^{-1}$ was found increased in $L^2$ and $L^3$ leaf samples by 22.98% and 25.51% respectively whereas it decreased in $L^1$ and $L^4$ leaf samples by 11.62% and 22.55% respectively. Thus the results clearly shows that the increase in total protein content is mainly contributed by α − helix and β − sheet of secondary structure of protein [17].

Table 4
Frequency assignment for secondary protein obtained by self deconvoluted spectra.

| Wavenumber ($cm^{-1}$) | Control | $L^1$ | $L^2$ | $L^3$ | $L^4$ |
|---|---|---|---|---|---|
| 1633 (β − sheet) | 1.478 ± 0.008 | 2.081 ± 0.003 +40.77 | 1.748 ± 0.011 +18.26 | 3.729 ± 0.014 +152.23 | 3.343 ± 0.010 +126.17 |
| 1648 (Random coil) | 2.253 ± 0.011 | 3.093 ± 0.016 +37.27 | 2.234 ± 0.007 −0.82 | 2.818 ± 0.012 +25.08 | 2.825 ± 0.009 +25.38 |
| 1656 (α − helix) | 1.034 ± 0.004 | 3.332 ± 0.005 +222.12 | 2.439 ± 0.004 +135.80 | 1.949 ± 0.005 +88.41 | 3.463 ± 0.002 +234.72 |
| 1666 (β − turn) | 1.391 ± 0.021 | 2.652 ± 0.018 +90.59 | 2.970 ± 0.009 +113.50 | 2.155 ± 0.006 +54.89 | 2.134 ± 0.008 +53.41 |
| 1673 (β − turn) | 0.999 ± 0.014 | 2.060 ± 0.012 +106.12 | 1.589 ± 0.024 +59.02 | 1.907 ± 0.020 +90.83 | 1.822 ± 0.014 +82.31 |
| 1684 (β − turn) | 2.177 ± 0.012 | 1.924 ± 0.016−11.62 | 2.678 ± 0.013 +22.98 | 2.732 ± 0.018 +25.51 | 1.686 ± 0.012−22.55 |

The values are the mean ± S.E for each group (n = 9). Comparisons were done by Students t-test. The degree of significance was $p < 0.05$.

Table 5
Pearson correlation matrix for variation in secondary structure protein of all leaf samples.

| Wavenumber ($cm^{-1}$) | 1633 | 1648 | 1656 | 1666 | 1673 | 1684 |
|---|---|---|---|---|---|---|
| 1633 | 1 | 0.994[a] | 0.140 | 0.924[b] | 0.972[a] | 0.860 |
| 1648 | 0.994[a] | 1 | 0.068 | 0.945[b] | 0.974[a] | 0.905[b] |
| 1656 | 0.140 | 0.068 | 1 | 0.149 | 0.219 | −0.275 |
| 1666 | 0.924[b] | 0.945[b] | 0.149 | 1 | 0.980[a] | 0.907[b] |
| 1673 | 0.972[a] | 0.974[a] | 0.219 | 0.980[a] | 1 | 0.871 |
| 1684 | 0.860 | 0.905[b] | −0.275 | 0.907[b] | 0.871 | 1 |

[a] Correlation is significant at the 0.01 level (2-tailed).
[b] Correlation is significant at the 0.05 level (2-tailed).

### 3.3. Pearson correlation coefficient matrix for secondary structure of protein

The Pearson's correlation coefficient matrix measures the strength of a linear relationship between any two variables on a scale of +1 (positive linear correlation) to −1 (negative linear correlation). In this study, the derived intensities of the secondary structure protein were used in calculating the correlation coefficient using the SPSS 16.0. The matrix of linear correlation coefficient is show in Table 5 which is significant at the 0.01 level (2-tailed). The correlation coefficient values vary from 0.140 between 1633 and 1656 $cm^{-1}$, to 0.980 between 1666 and 1673 $cm^{-1}$. The positive correlation exist between 1633−1648 $cm^{-1}$ and 1633−1673 $cm^{-1}$ clearly indicates β − sheet increases with increase in random coil and β − turn vice versa. Also positive correlations exist between the wavenumber 1673−1648 $cm^{-1}$ and 1673−1666 $cm^{-1}$ corresponds to increase in β − turn of secondary structure of protein with random coil and vice versa. There is no negative correlation between any of the secondary structures of protein which indicates α − helix; β − sheet and β − turn does not increase at the expenses of one another. The wavenumber 1656 $cm^{-1}$ corresponds to α − helix of protein secondary structure does not have any impact due to the other protein secondary structures [18].

Table 6
Variation of protein secondary structure in leaf samples are calculated using varimax rotated factor analysis of principal component extraction method.

| Component | Rotation sums of squared loadings | | |
|---|---|---|---|
| | Total | % of Variance | Cumulative % |
| 1 | 4.737 | 78.943 | 78.943 |
| 2 | 1.150 | 19.172 | 98.115 |

Varimax rotated component matrix

| Samples | Component | |
|---|---|---|
| | 1 | 2 |
| W1633 | 0.976 | 0.098 |
| W1648 | 0.990 | 0.023 |
| W1656 | 0.051 | 0.998 |
| W1666 | 0.976 | 0.092 |
| W1673 | 0.984 | 0.169 |
| W1684 | 0.938 | −0.328 |

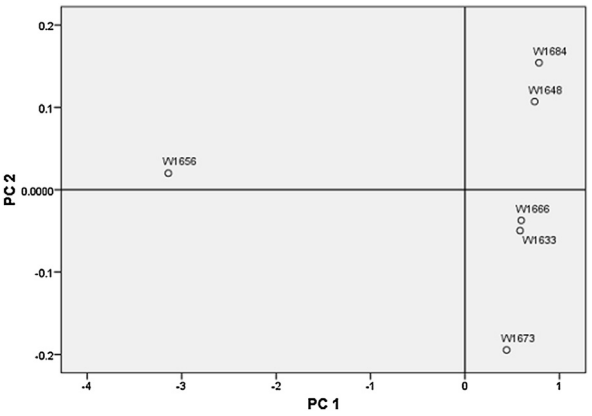


Fig. 6. Principle component analysis explained variance in secondary structure protein of control, $L^1$, $L^2$, $L^3$ & $L^4$ leaf samples.

### 3.4. Principal component analysis for variation in secondary structure of protein

Further principal component analysis using SPSS 16.0 software is performed for understanding the protein secondary structure variation among the leaf samples obtained by seed presoaked with bulk and nano zinc oxide suspensions compared with control sample. The results in Table 6 shows that the variation of secondary structure of protein due to the metal treatment is calculated using varimax rotated factor analysis of principal component extraction method.

Factor analysis or principle component analysis is a useful tool in the examination of multivariate data (Fig. 6). Using rotated factor loading and commonalities varimax rotation analysis, information about the main factors in the studied samples was obtained. The successive factors account for decreasing amounts of residual variance using two factors (varimax rotation) for the wavenumbers 1633, 1648, 1656, 1666, 1673 and 1684 $cm^{-1}$ assigned to protein secondary structure of leaf samples. The cumulative percentage of explained variance in wavenumbers of secondary structure of protein of all leaf samples is 98.115%. The main factor (>0.6) account for 78.943% of the total data variance, the variation of secondary structure of protein was established by accounting the wavenumber 1633, 1648, 1666, 1673 and 1684 $cm^{-1}$. Factor 2

accounts for 19.172% which includes the 1656 $cm^{-1}$ of protein secondary structure. These results explain that $\alpha$ – helix of protein secondary structure might not required for studying the variation in protein secondary structures of leaf samples obtained by seed presoaking with bulk and nano zinc oxide suspensions [19].

## 4. Conclusions

The effect of presoaking peanut seeds in bulk and nano form of zinc oxide suspension was studied extensively. The synthesized zinc oxide nanoparticle was phase confirmed with XRD results and it measures average particle size of 23.9 nm. The SEM, TEM and AFM images confirms the uniformity and particle size of nanoparticles. The FT-IR results, band area calculation and calculated mean intensity ratios of peanut plant leaves collected after 30 days of growth period explains that zinc oxide nanoparticle has considerable effect on the protein, chlorophyll, carbohydrate and other biochemical constituents when applied through presoaking the peanut plant seeds in zinc oxide bulk and nanoparticle suspensions. The Fourier self-deconvolution and second derivative spectra explained that $\beta$ – sheet, $\beta$ – turn, random coil and $\alpha$ – helix of protein secondary structure varied to greater extent in all leaf samples compared to control sample. The correlation matrix for secondary structures of protein shows that there is no variation in $\alpha$ – helix with respect to other protein secondary structure of leaf samples. The PCA analysis supports the results obtained in correlation matrix where $\alpha$ – helix does not group with other protein secondary structure.

## References

[1] M. Farooq, A. Wahid, K.H.M. Siddique, J. Plant Nutr. Soil Sci. 12 (2012) 125–142.
[2] M. Imtiaz, A. Rashid, P. Khan, M.Y. Memon, M. Aslam, Pak. J. Bot. 42 (2010) 2565–2578.
[3] D.T. Clarkson, J.B. Hanson, Annu. Rev. Plant Physiol. 31 (1980) 239–298.
[4] B. Subash, B. Krishnakumar, M. Swaminathan, M. Shanthi, Langmuir 29 (3) (2013) 939–949.
[5] J. Jayabharathi, V. Thanikachalam, V. Kalaiarasi, K. Jayamoorthy, Spectrochim. Acta Part A 118 (2014) 182–186.
[6] B. Subash, A. Senthilraja, P. Dhatshanamurthi, M. Swaminathan, M. Shanthi, Spectrochim. Acta A 115 (2013) 175.
[7] J. Jayabharathi, V. Thanikachalam, K. Jayamoorthy, Spectrochim. Acta A 95 (2012) 143–147.
[8] P. Saravanan, K. Jayamoorthy, S.A. Kumar, Sensors Actuators B Chem. 221 (2015) 784–791.
[9] C. Karunakaran, J. Jayabharathi, K. Jayamoorthy, Measurement 46 (2013) 3883–3886.
[10] C. Karunakaran, J. Jayabharathi, R. Sathishkumar, K. Jayamoorthy, K. Vimal, Spectrochim. Acta Part A 115 (2013) 488–492.
[11] I. Cakmak, H. Marschner, J. Plant Physiol. 132 (1988) 356–361.
[12] T.N.V.K.V. Prasad, P. Sudhakar, Y. Sreenivasulu, P. Latha, V. Munaswamy, K. Raja Reddy, T.S. Sreeprasad, P.R. Sajanlal, T. Pradeep, J. Plant Nutr. 35 (2012) 905–927.
[13] K. Maroufi, H.A. Farahani, A.M. Aghdam, Adv. Environ. Biol. 5 (2011) 3747–3750.
[14] C. Karunakaran, J. Jayabharathi, K. Jayamoorthy, P. Vinayagamoorthy, Mater. Express 4 (2014) 279–292.
[15] M. Ashraf, M.R. Foolad, Adv. Agron. 88 (2005) 223–271.
[16] L. Zheng, F.S. Hong, S.P. Lu, C. Liu, Biol. Trace Elem. Res. 104 (2005) 83–91.
[17] A. Dogan, G. Siyakus, F. Severcan, Food Chem. 100 (2007) 1106–1114.
[18] L.J. Boucher, H.H. Strain, J.J. Katz, J. Am. Chem. Soc. 88 (1966) 1341.
[19] Z.L. Wei, L. Dong, Z.H. Tian, Pak. J. Bot. 41 (2009) 1743–1750.